COBEM 2023 27TH INTERNATIONAL CONGRESS OF MECHANICAL ENGINEERING

ABCM Brazilian Society of Mechanical Sciences and Engineering
27th ABCM International Congress of Mechanical Engineering
December 04-08, 2023, Florianópolis-SC, Brazil

COB-2023-2129
COMPARISON OF THE PERFORMANCES OF THE WIDE-BAND BASED WEIGHTED-SUM-OF-GRAY-GASES AND BOX MODELS IN THE CALCULATION OF NON-GRAY BOUNDARIES AT HIGH PRESSURES

Roberta Juliana Collet da Fonseca
Guilherme Crivelli Fraga
Francis Henrique Ramos França
Department of Mechanical Engineering, Federal University of Rio Grande do Sul, Porto Alegre, Brazil
roberta.fonseca@ufrgs.br
guilhermecfraga@ufrgs.br
frfranca@mecanica.ufrgs.br

Abstract. *Thermal radiation is a mechanism of heat transfer that generally dominates the heat exchange in flames, furnaces and fires at high temperatures. In combustion problems, a difficulty is that typical products of the burning process (water vapor, carbon dioxide and soot) participate in the thermal exchange, absorbing, emitting or scattering radiation. In most applications, the boundaries are treated as black, which allows the decoupling of the spectral integration of the medium in relation to the surface, so that the gas models can be developed independently of the conditions at the boundary. Alternatively to the spectral integration of the radiative transfer equation (RTE) through the line-by-line (LBL) method, the spectral models reduce the computational cost, keeping the accuracy of the solution. In this paper, the wide-band based weighted-sum-of-gray-gases (WBW) model solves the radiative transfer of a participating medium with a H_2O-CO_2 mixture confined by non-gray walls. In this model, the spectrum is divided into bands, and the standard weighted-sum-of-gray-gases (WSGG) model is used to solve each segment. The total pressure of the system assumes values between 1 atm and 20 atm. Results show that the WBW model has a higher accuracy than conventional box models, with maximum errors of* 4 %.

Keywords: *thermal radiation, wide-band models, box models, non-gray surfaces, high pressures*

1. INTRODUCTION

Recent efforts to decrease their harmful effects on the environment have made applications for combustion at high pressure scenarios quite popular. Rockets, gas turbines, and piston engines are only a few examples of combustion devices that work at pressures higher than atmospheric (Modest and Haworth, 2016). The use of oxy-combustion for carbon capture and storage is a further use of high pressure combustion, with the primary objective of reducing atmospheric CO_2 emissions (Wall *et al.*, 2011). A few of the combustion byproducts are also participating gases, such water vapor and carbon dioxide, which can emit, absorb, or scatter thermal radiation. In this framework, it is crucial to understand how to accurately calculate the radiative heat transfer in participating medium in order to enhance the combustion processes, especially the systems that operate at high pressures, which are more expensive than those at atmospheric pressure.

The total pressure of the system influences on thermal radiation, which is often the main mechanism of heat transfer in combustion processes due to the high temperatures involved. This importance becomes even greater for high pressures, since the radiation absorption increases with the total pressure, which, in turn, also affects the chemical reactions (Chen *et al.*, 2007). Soot radiation also affects the chemical reactions and has a significant dependence on the pressure, mainly through increases in the soot formation (Modest and Haworth, 2016).

The radiative transfer equation (RTE) is the mathematical expression that governs the heat transfer by thermal radiation in a participating medium. The existence of high-resolution spectral databases, such as HITEMP (high-temperature molecular spectroscopic database) (Rothman *et al.*, 2010), which offer details on the absorption coefficient of various chemical species, makes it possible to achieve the RTE solution through line-by-line (LBL) integration (Taine, 1983), despite the fact that it requires a long calculation process. Alternatively to the LBL integration, there is the weighted sum-of-gray-gases (WSGG) model (Hottel and Sarofim, 1967), which replaces the highly irregular behavior of the absorption coefficient of a gas by some equivalent gray gases with uniform absorption coefficients plus transparent windows. Each gray gas is represented by a weighting factor, which, together with the absorption coefficient, are determined by fitting total emittance data calculated through the radiative properties present in the databases. The WSGG model has generally worked effectively under atmospheric pressure circumstances (Dorigon *et al.*, 2013; Bordbar *et al.*, 2014; Selhorst *et al.*, 2022), but there are few studies using coefficients generated through emittance data at elevated pressures (Coelho and França, 2018; Bordbar *et al.*, 2021; Fonseca *et al.*, 2023b). There are some studies in which the researchers have attempted to apply these parameters to high pressure scenarios due to the dearth of WSGG coefficients at pressures above the atmospheric level, but their efforts

have often failed (Kez *et al.*, 2016; Chu *et al.*, 2017). Other spectral models, including the spectral-line based WSGG (SLW), statistical narrow-band (SNB), statistical narrow-band correlated-k (SNBCK), and full-spectrum correlated-k (FSCK) models, were also extended to high pressure scenarios. The results were found to be satisfactorily accurate when compared to the benchmark solution (Chu *et al.*, 2016, 2017).

In the spectral modeling field, the boundaries of the domain are typically represented as black surfaces. In order to develop spectral gas models regardless of the characteristics at the boundaries, this assumption enables the decoupling of the spectral integration of the medium in respect to the surface. The investigation of radiative exchanges between participating gases and non-gray surfaces has received minimal attention in the literature, in contrast to research in which the boundaries are black. In order to take into consideration the reflection of the radiation intensity on the walls, which is given as a function of the intensity incident on them (which, in turn, depends on the properties of the medium), the RTE must be solved iteratively at the non-gray boundaries. Due to the fact that the intensities at the boundary are known on black surfaces and the RTE may thus be solved in a single step, this feature makes the calculation computationally more expensive. Denison and Webb (1994), Solovjov *et al.* (2013), Fonseca *et al.* (2018), Liu *et al.* (2019), Fonseca *et al.* (2021) and Fonseca *et al.* (2022) are some of the authors who proposed formulations for the treatment of non-gray surfaces in the context of the spectral models.

In the present paper, the spectral integration of the RTE is solved using the wide-band based weighted-sum-of-gray-gases (WBW) model (Fonseca *et al.*, 2023a). In order to enhance the performance of the standard WSGG model, the WBW model seeks to refine the spectrum by segmenting it into a number of spectral bands and using it to solve each one of these intervals. The proposed method is used to solve the radiative heat transfer between a participating medium—composed of a H_2O-CO_2 mixture—and the non-gray walls that delimit the domain. The total pressure of the one-dimensional system is varied between the values of 1 atm and 20 atm. It is the first time that the effects of non-gray boundaries and elevated pressures are combined and solved through the WBW model. The accuracy of the results obtained with the proposed methodology are compared with the LBL integration and with a box model, which uses a gray approach to describe the radiative properties of the participating gases.

2. RADIATION MODELING

In this section, the concepts and theoretical formulation that govern the heat transfer by thermal radiation are briefly presented.

2.1 The line-by-line method

The radiative transfer equation (RTE) is a first-order integral-differential equation with respect to spectral intensity that governs the heat transfer by thermal radiation, and its solution depends on the spectral intensity at a specific location in the domain. Neglecting the scattering effects, the RTE for a participating medium, in a given path s, is written as (Modest, 2013; Howell *et al.*, 2016)

$$\frac{\mathrm{d}I_\eta}{\mathrm{d}s} = -\kappa_\eta I_\eta + \kappa_\eta I_{b\eta} \,. \tag{1}$$

In the above equation, I_η is the spectral radiation intensity, κ_η is the spectral absorption coefficient of the participating medium and $I_{b\eta}$ is the blackbody spectral radiation intensity, which is computed from the Planck's distribution function for a given temperature T and wavenumber η.

Assuming a diffuse and non-gray wall at $x = 0$, the boundary condition associated to Eq. (1) is given by

$$I_\eta\Big|_{x=0} = I_{\eta,0} = \varepsilon_\eta I_{b\eta,0} + (1-\alpha_\eta)\overline{I_{\eta,i}} \,, \tag{2}$$

where ε_η and α_η are the spectral emissivity and the spectral absorptivity of the surface, respectively. The terms $I_{b\eta,0}$ and $\overline{I_{\eta,i}}$ are the spectral blackbody intensity evaluated at the left boundary (i.e., $x = 0$) and the average spectral intensity that arrives on the wall, respectively. The subindex i in the term $\overline{I_{\eta,i}}$ represents the incident intensity on the wall, which is computed as

$$\overline{I_{\eta,i}} = \frac{1}{\pi}\int_0^{2\pi} (I_{\eta,i}\cos\theta_i)\mathrm{d}\omega_i \,, \tag{3}$$

in which $I_{\eta,i}$ is the spectral intensity that is incident on the wall from the direction $\mathrm{d}\omega_i$. For perfectly diffuse surfaces, $\varepsilon_\eta = \alpha_\eta$.

The total radiative intensity and the spectral intensity at the boundary can be solved integrating these quantities over the entire spectrum, such as $I = \int_0^\infty I_\eta \,\mathrm{d}\eta$ and $I_0 = \int_0^\infty I_{\eta,0}\,\mathrm{d}\eta$. In this way, the integrated boundary condition becomes

$$I_0 = \varepsilon I_{b,0} + (1-\alpha)\overline{I_i} \,, \tag{4}$$

where the blackbody radiative intensity on the left wall and the incident intensity are calculated as $I_{b,0} = \int_0^\infty I_{b\eta,0}\,\mathrm{d}\eta$ and $\overline{I_i} = \int_0^\infty \overline{I_{\eta,i}}\,\mathrm{d}\eta$, respectively. The total emissivity, ε, and the total absorptivity, α, are computed, respectively, as

$$\varepsilon = \frac{\int_0^\infty \varepsilon_\eta I_{b\eta,0}\,\mathrm{d}\eta}{I_{b,0}}\,, \tag{5}$$

$$\alpha = \frac{\int_0^\infty \alpha_\eta \overline{I_{\eta,i}}\,\mathrm{d}\eta}{\overline{I_i}}\,. \tag{6}$$

The radiative heat flux, q_r, and radiative heat source, S_r, at each location in the domain can be determined by integrating the RTE and solving the spectral radiation intensities for a set of directions. These quantities can be calculated by the following equations:

$$q_r(x) = \sum_{l=1}^{n_d} \int_\eta \left\{ 2\pi\mu_l\omega_l \left[I^+_{\eta,l}(x) - I^-_{\eta,l}(x) \right] \right\} \mathrm{d}\eta\,, \tag{7}$$

$$S_r(x) = \sum_{l=1}^{n_d} \int_\eta \left\{ 2\pi\kappa_\eta\omega_l \left[I^+_{\eta,l}(x) + I^-_{\eta,l}(x) \right] - 4\pi\kappa_\eta I_{b\eta}(x) \right\} \mathrm{d}\eta\,, \tag{8}$$

in which n_d is the number of directions in which the integration of the RTE is performed. The terms μ_l and ω_l are the direction cosine and the weight of the Gauss-Legendre quadrature, and $I^+_{\eta,l}$ and $I^-_{\eta,l}$ are the forward and backward spectral radiation intensities, respectively.

2.2 The box model

In the present paper, the full spectrum is divided into a set of discrete bands. For comparison purposes with the proposed method, a stepwise-gray model, which is a straightforward and practical wide-band spectral model, was also implemented and tested. In this framework, a very simple box model, in which the band is approximated by a rectangular box of width $\Delta\eta_m$ and height κ_P was employed, which means that the first parameter represents the size of the spectral band and the second one the absorption coefficient corresponding to that segment. So, for each spectral band, an average value of absorption coefficient was computed. Problems involving non-gray radiation have been resolved using a variety of stepwise-gray spectral models (Edwards *et al.*, 1967; Modest and Sikka, 1992; Kaminski *et al.*, 1995; Mazumder and Modest, 1999).

The Planck-mean absorption coefficient, which typically characterizes the radiative heat loss from an optically thin gas, quantifies the total emission from a medium. Furthermore, the Planck-mean absorption coefficient serves as a helpful reference in a series of approximation techniques, such as the semi-gray approximation (Modest, 2013). Once the lower and upper bounds for each spectral band have been established, the Planck-mean absorption coefficient of each segment, κ_P, can be computed as (Modest, 2013; Howell *et al.*, 2016)

$$\kappa_P = \frac{\int_{\Delta\eta_m} \kappa_\eta I_{b\eta}\,\mathrm{d}\eta}{\int_{\Delta\eta_m} I_{b\eta}\,\mathrm{d}\eta}\,, \tag{9}$$

where $\Delta\eta_m$ is an arbitrary band in which the radiation spectrum was divided. In this paper, one value of κ_P for each one of the five spectral bands was determined. The set of these five values of κ_P configures the solution obtained through the box model discussed in Chapter 4.

2.3 The wide-band based weighted-sum-of-gray-gases model

The proposed methodology consists of applying the wide-band based WSGG (WBW) model (Fonseca *et al.*, 2023a) to solve the heat exchanges between a participating medium and the non-gray boundaries that enclose this system. The WBW model is a global spectral model in which the spectrum is divided into a set of discrete bands and the standard WSGG model is used to solve the individual contribution of each segment.

Under the assumptions of the WBW model, the RTE, for an arbitrary spectral band m and a gray gas j, is given by

$$\frac{\mathrm{d}I_{j,m}}{\mathrm{d}x} = -\kappa_{pj,m}p_a I_{j,m} + \kappa_{pj,m}p_a a_{j,m} f_m I_b\,, \tag{10}$$

in which $\kappa_{pj,m}$ is the pressure-absorption coefficient, p_a is the partial pressure of the absorbing-emitting species, $I_{j,m}$ is the partial intensity corresponding to the j-th gray gas, $a_{j,m}$ is the temperature coefficient, f_m is the fraction of blackbody

energy emitted from the band $\Delta\eta_m$ and I_b is the total blackbody radiation intensity. The parameters $\kappa_{pj,m}$ and $a_{j,m}$ can be determined by fitting LBL emittance data through the high-resolution spectral databases, such as HITEMP 2010.

The RTE of Eq. (10) is subjected to the following boundary condition:

$$I_{j,m}\Big|_{x=0} = \varepsilon_m a_{j,m,0} f_{m,0} I_{b,0} + (1-\alpha_m)\overline{I_{j,i,m}}\,, \tag{11}$$

where ε_m and α_m are the partial emissivity and the partial absorptivity of the surface, respectively, of the spectral band m. The insertion of the term $f_{m,0}$ in the above equation is due to the fact that it is necessary to account for the fraction of blackbody energy that is emitted in that spectral band. Again, the subindex i represents the incident intensity for an arbitrary gray gas j. The emissivity and absorptivity for an arbitrary band m are expressed as

$$\varepsilon_m = \frac{\int_{\Delta\eta_m} \varepsilon_{\eta,m} I_{b\eta,0} \mathrm{d}\eta}{a_{j,0} I_{b,0}}\,, \tag{12}$$

$$\alpha_m = \frac{\int_{\Delta\eta_m} \alpha_{\eta,m} \overline{I_{\eta,i,m}} \mathrm{d}\eta}{\overline{I_i}}\,. \tag{13}$$

Finally, after solving Eq. (10), the calculation of the radiative heat flux and radiative heat source for each spectral band follows the equations below:

$$q_r(x) = \sum_{m=1}^{n_b}\sum_{l=1}^{n_d}\sum_{j=1}^{J}\left\{2\pi\mu_l\omega_l\left[I^+_{j,l,m}(x) - I^-_{j,l,m}(x)\right]\right\}, \tag{14}$$

$$S_r(x) = \sum_{m=1}^{n_b}\sum_{l=1}^{n_d}\sum_{j=1}^{J}\left\{2\pi\kappa_{pj,m}p_a\omega_l\left[I^+_{j,l,m}(x) + I^-_{j,l,m}(x)\right] - 4\pi\kappa_{pj,m}p_a a_{j,m} f_m I_b(x)\right\}, \tag{15}$$

in which n_b is the number of bands in which the spectrum was divided, and $I^+_{j,l,m}$ and $I^-_{j,l,m}$ are the intensities in the forward and backward directions of the j-th gray gas.

3. PROBLEM DESCRIPTION AND SOLUTION METHODOLOGY

The radiative heat transfer in a one-dimensional media slab is studied in this paper. The participating medium, which is composed of a non-homogeneous and non-isothermal mixture of water vapor and carbon dioxide, is confined by two diffuse and non-gray walls that make up the 1D domain. Chapter 4 provides a description of the mole fraction and temperature profiles that are assessed. The total pressure of the system assumes the values of 1 atm, 10 atm and 20 atm; the distance between the plates is $L = 1$ m. Figure 1 depicts the domain under study. The spectral integration of the RTE was solved using the WBW model and the directional integration was completed using the discrete ordinates method (DOM) for 8 directions, in accordance with the parameters outlined by Lathrop and Carlson (1964). 200 identically sized cells make up the spatial domain. The selection and usage of these directional and spatial discretization parameters were thoroughly detailed in Fonseca *et al.* (2023a), and it was shown to be suitable for simulations under the same physical conditions as those investigated in this paper. The details about the generation of the absorption spectra of H_2O and CO_2 can be found in Dorigon *et al.* (2013), and Coelho and França (2018).

A five-band stepwise variation provides the spectral emissivity distribution for the non-gray walls: $\varepsilon_\eta = 0.5$ for $0\,\mathrm{cm}^{-1} < \eta < 1000\,\mathrm{cm}^{-1}$; $\varepsilon_\eta = 0.6$ for $1000\,\mathrm{cm}^{-1} < \eta < 2600\,\mathrm{cm}^{-1}$; $\varepsilon_\eta = 0.7$ for $2600\,\mathrm{cm}^{-1} < \eta < 4400\,\mathrm{cm}^{-1}$; $\varepsilon_\eta = 0.8$ for $4400\,\mathrm{cm}^{-1} < \eta < 6000\,\mathrm{cm}^{-1}$; and $\varepsilon_\eta = 0.9$ for $6000\,\mathrm{cm}^{-1} < \eta < 25\,000\,\mathrm{cm}^{-1}$. Although the proposed methodology is not limited to this case, both walls present the same spectral emissivity profile. The WBW method and a box model were used to solve the spectral integration of the problem, and the results were compared against LBL calculations. For $p = 1$ atm, the set of correlations obtained with the WBW model by Fonseca *et al.* (2023a) was used, with four gray gases in each spectral band. For the other values of total pressure, the WBW coefficients generated by Fonseca *et al.* (2023b) were employed, also

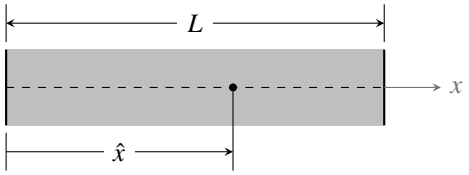

Figure 1. Representation of the one-dimensional domain.

considering that each band has four gray gases. The spectrum was segmented into the identical regions that were indicated in the description of the surfaces' emissivity profiles. The results, which were determined in terms of the radiative heat flux and radiative heat source, are presented in the following section.

4. RESULTS AND DISCUSSION

The proposed methodology is tested through three different profiles of temperature and mole fraction of the participating species. The temperature profile are given by the following set of equations:

$$T(\hat{x}) = 400 + 1400\sin^2(\pi\hat{x})\,, \tag{16}$$

$$T(\hat{x}) = 400 + 1400\sin^2(2\pi\hat{x})\,, \tag{17}$$

$$T(\hat{x}) = \begin{cases} 880 + 920\sin^2(2\pi\hat{x}), \text{if } \hat{x} \leq 0.25 \\ 400 + 1400\left\{1 - \sin^{3/2}[2\pi/3(\hat{x} - 0.25)]\right\}, \text{if } \hat{x} > 0.25 \end{cases}, \tag{18}$$

where $\hat{x} = x/L$ is a dimensionless quantity that represents the distance from the left wall. The mole fraction profiles of carbon dioxide, Y_c, follow the equations below:

$$Y_c(\hat{x}) = 0.1\sin^2(\pi\hat{x})\,, \tag{19}$$

$$Y_c(\hat{x}) = 0.1\sin^2(2\pi\hat{x})\,, \tag{20}$$

$$Y_c(\hat{x}) = \begin{cases} 0.1\sin^2(2\pi\hat{x}), \text{if } \hat{x} \leq 0.25 \\ 0.1\left\{1 - \sin^{3/2}[2\pi/3(\hat{x} - 0.25)]\right\}, \text{if } \hat{x} > 0.25 \end{cases}. \tag{21}$$

In the above equations, the maximum values of temperature and CO_2 mole fraction are 1800 K and 0.1, respectively; the average temperature and mole fraction are 1100 K and 0.05, respectively. Equations (16) and (19) represent profiles with simple symmetry in relation to the x- axis, with a peak located at the center of the domain, (i.e., at $\hat{x} = 0.5$). Equations (17) and (20) are profiles with double symmetry in relation to the x-axis, with two peaks, at positions $\hat{x} = 0.25$ and $\hat{x} = 0.75$. Equations (18) and (21) represent profiles without symmetry in relation to the x-axis, with a peak at $\hat{x} = 0.25$. In the three mole fraction profiles, $Y_w = 2Y_c$, in which Y_w is the H_2O mole fraction. Figure 2 shows these profiles.

In the present paper, the type of symmetry in relation to the x-axis (or the absence of it) is combined in order to compose the test cases under study. For instance, in Case 1, the temperature and mole fraction profiles are described by the combination of Eqs. (16) and (19). Analogously, Cases 2 and 3 are described by Eqs. (17) and (20), and Eqs. (18) and (21), respectively. The cases tested here follow similar conditions to those presented in Fonseca *et al.* (2023b), but with a domain bounded by non-gray walls.

The accuracy of the test cases is evaluated through comparisons the LBL benchmark solution and the approach used to the box model. In this framework, a normalized percentage deviation was defined according to the equation below:

$$\delta\phi = \frac{|\phi_{\text{LBL}} - \phi_{\text{app}}|}{\max(|\phi_{\text{LBL}}|)}\,, \tag{22}$$

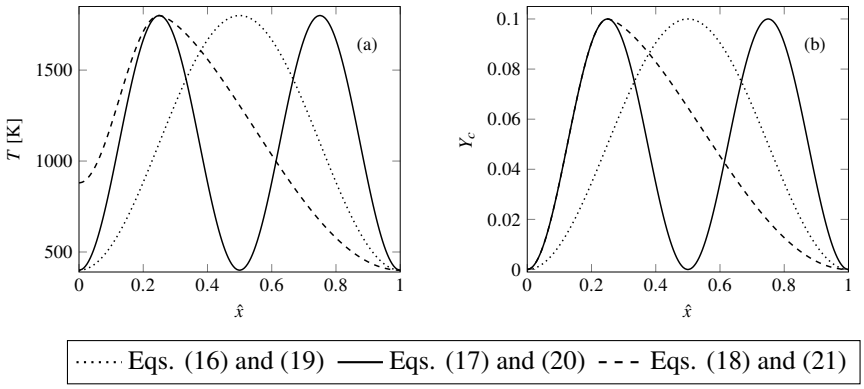

Figure 2. Profiles tested in this paper: (a) temperature profile; (b) CO_2 mole fraction profile.

in which ϕ is either the radiative heat flux or radiative heat source, the subscripts "LBL" and "app" represent the LBL and the tested approach (the WBW or the box models in this study), and the $\max(|\phi_{\text{LBL}}|)$ is the maximum absolute value of ϕ. Later, the subscripts "max" and "avg" will be used to designate the maximum and average deviations, respectively.

Figure 3 shows the results of radiative heat flux and radiative heat source for temperature and CO_2 mole fraction profiles of Eqs. (16) and (19), i.e., Case 1. As it can be seen in the figure, the system is subjected to the total pressures of 1 atm, 10 atm and 20 atm, and the WBW model was compared against the LBL integration and a box model. As expected, for all the total pressure values that were tested, it was verified a better performance of the WBW model in relation to the box model. The magnitudes of these comparisons can be observed in Table 1, which shows the maximum and average percentages deviations between the tested approaches regarding the LBL benchmark solution. So, for $p = 1$ atm, one can observe that the maximum errors in relation to the LBL solution obtained with the proposed method were 2.94 % for the radiative heat flux and 3.33 % for the radiative heat source, against 89.29 % (q_r) and 77.3 % (S_r) with the other approach. For $p = 10$ atm, the maximum errors were 23.18 %, for S_r with the box model, and 2.09 %, for q_r with the WBW solution. For the pressure of 20 atm, the maximum deviations were observed for the radiative heat source for both solutions, being 17.66 % (box model) and 2.27 % (WBW model).

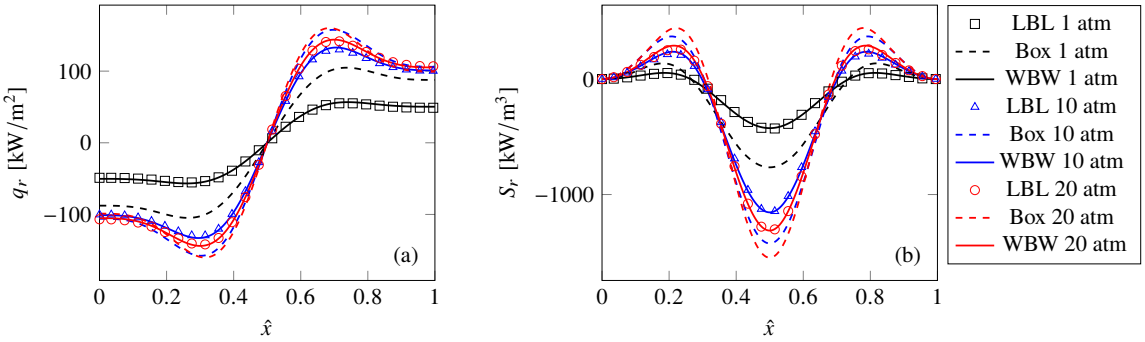

Figure 3. Results for Case 1: (a) radiative heat flux; (b) radiative heat source.

The results of q_r and S_r for Case 2 (Eqs. (17) and (20)) are depicted in Fig. 4. As in the previous case, the figure presents the curves of the results for the three values of total pressure that were investigated with the LBL, WBW and box solutions. Again comparing the two tested approaches, the WBW model was presented as the best option to solve the heat transfer, once the proposed method reached maximum deviations of 3.25 % and 3.68 % for the radiative heat flux and radiative heat source, respectively, regarding the LBL solution, for $p = 1$ atm. The box model, in turn, led to maximum errors of 84.47 % and 73.37 % for q_r and S_r, respectively, demonstrating, again, low accuracy to describe the behavior of the solution. For $p = 10$ atm, the maximum deviations were 22.9 % (q_r) and 30.73 % (S_r), with the box model, and 2.72 % (q_r) and 2.36 % (S_r) through the WBW model. The maximum errors obtained for the pressure of 20 atm were found for the radiative heat source with both approaches, with the magnitudes of 4.22 % and 27.81 % with WBW and box models, respectively.

Figure 5 depicts the radiative heat flux and radiative heat source for Case 3, whose temperature and CO_2 mole fraction profiles are given by Eqs. (16) and (19), respectively. Similarly to the previous results, in Case 3 the behavior of the solution with the WBW model presented a good match in relation to the LBL integration, with maximum deviations of 3.27 %, for q_r, and 4.35 %, for S_r, when $p = 1$ atm. However, with the box model, the maximum errors were 84 %, for q_r, and 73.3 %, for S_r. For the other values of total pressure, the box model also presented the worst performance: for $p = 10$ atm, the maximum errors were obtained for q_r for the box model, whose magnitude was 33.75 %, and for S_r for the WBW model, with 2.97 %; for 20 atm, these values 23 % (q_r with box model) and 2.8 % (S_r with WBW model).

For all cases evaluated in the present study, the WBW model presented a good agreement in relation to the LBL

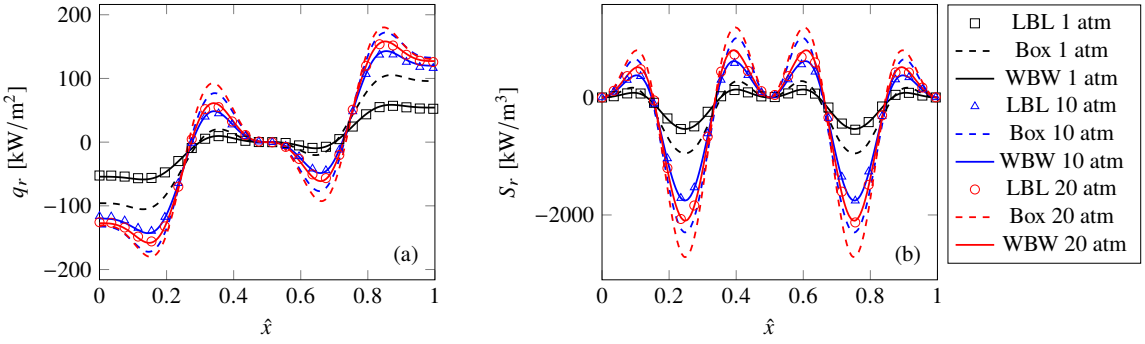

Figure 4. Results for Case 2: (a) radiative heat flux; (b) radiative heat source.

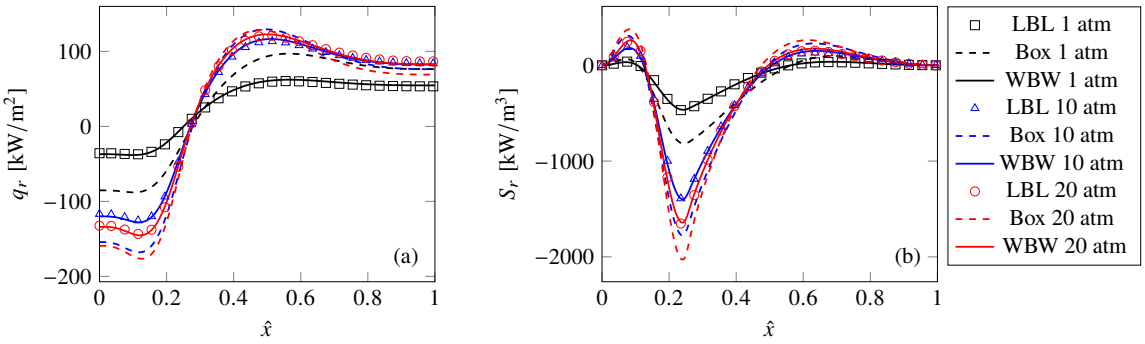

Figure 5. Results for Case 3: (a) radiative heat flux; (b) radiative heat source.

Table 1. Maximum and average normalized deviations of q_r and S_r between the LBL solution and the tested approaches.

	LBL method × Box model [%]				LBL method × WBW model [%]			
	$(\delta q_r)_{\max}$	$(\delta q_r)_{\text{avg}}$	$(\delta S_r)_{\max}$	$(\delta S_r)_{\text{avg}}$	$(\delta q_r)_{\max}$	$(\delta q_r)_{\text{avg}}$	$(\delta S_r)_{\max}$	$(\delta S_r)_{\text{avg}}$
				p = 1 atm				
Case 1	89.29	67.89	77.31	28.04	2.94	1.78	3.33	1.10
Case 2	84.47	41.71	73.37	27.21	3.25	1.39	3.68	1.41
Case 3	83.99	50.15	73.29	21.63	3.27	1.93	4.35	1.03
				p = 10 atm				
Case 1	21.32	11.88	23.18	9.43	2.09	0.97	2.03	0.81
Case 2	22.90	13.19	30.73	14.14	2.72	1.23	2.36	0.90
Case 3	33.75	12.14	27.09	6.97	2.51	1.37	2.97	0.75
				p = 20 atm				
Case 1	13.77	6.94	17.66	8.02	1.20	0.70	2.27	0.83
Case 2	21.97	9.77	27.81	12.43	2.55	0.88	4.22	1.32
Case 3	22.99	10.40	22.28	5.42	2.56	1.24	2.81	0.66

integration, while the box model proved inadequate to describe the radiative heat transfer. Although, with the increase in the total pressure, both models have improved their performances, the box model, in its best scenario, still presented errors of the order of 20 %, which demonstrates the effectiveness and accuracy of the proposed methodology in the sense of correctly solving the problem.

5. CONCLUSIONS

The WBW model was presented in this paper to describe the radiative transfer in scenarios with non-gray boundaries and pressures above the atmospheric. The WBW correlations used in the numerical simulations were generated by Fonseca *et al.* (2023a), for 1 atm, and Fonseca *et al.* (2023b), for 10 atm and 20 atm. The participating medium was composed of a non-homogeneous mixture of water vapor and carbon dioxide, confined by non-gray walls. The application of the proposed formulation led to satisfactory results regarding the LBL solution, with maximum errors of 4 %. The WBW model has also proven to be a better alternative than a gray approach typical of a box model. As potential directions for future research, an option is to evaluate more realistic emissivity profiles and to find other ways to divide the spectrum into bands without the need for them to coincide with the spectral emissivity distribution. In addition, seeking to optimize the number of gray gases in each spectral band, in order to obtain even more accurate results and with less computational effort, is also another alternative to try to improve the proposed method in future publications.

6. ACKNOWLEDGEMENTS

Authors RJCF and FHRF thank CNPq (Conselho Nacional de Desenvolvimento Tecnológico e Científico) for her postdoctoral fellowship and his research grant 302686/2017-7, respectively.

7. REFERENCES

Bordbar, H., Coelho, F.R., Fraga, G.C., França, F.H. and Hostikka, S., 2021. "Pressure-dependent weighted-sum-of-gray-gases models for heterogeneous CO_2-H_2O mixtures at sub- and super-atmospheric pressure". *Journal of Heat and Mass Transfer*, Vol. 173, p. 121207.

Bordbar, M.H., Wecel, G. and Hyppänen, T., 2014. "A line by line based weighted sum of gray gases model for inhomogeneous CO_2-H_2O mixture in oxy-fired combustion". *Combustion and Flame*, Vol. 161, No. 9, pp. 2435–2445.

Chandrasekhar, S., 1960. *Radiative Transfer*. Dover Publications.

Chen, Z., Qin, X., Xu, B., Ju, Y. and Liu, F., 2007. "Studies of radiation absorption on flame speed and flammability limit of CO_2 diluted methane flames at elevated pressures". *Proceedings of the Combustion Institute*, Vol. 31, No. 2, pp. 2693–2700.

Chu, H., Consalvi, J.L., Gu, M. and Liu, F., 2017. "Calculations of radiative heat transfer in an axisymmetric jet diffusion flame at elevated pressures using different gas radiation models". *Journal of Quantitative Spectroscopy and Radiative Transfer*, Vol. 197, pp. 12–25.

Chu, H., Gu, M., Consalvi, J.L., Liu, F. and Zhou, H., 2016. "Effects of total pressure on non-grey gas radiation transfer in oxy-fuel combustion using the LBL, SNB, SNBCK, WSGG, and FSCK methods". *Journal of Quantitative Spectroscopy and Radiative Transfer*, Vol. 172, pp. 24–35.

Coelho, F.R. and França, F.H., 2018. "WSGG correlations based on HITEMP2010 for gas mixtures of H_2O and CO_2 in high total pressure conditions". *International Journal of Heat and Mass Transfer*, Vol. 127, pp. 105–114.

Denison, M.K. and Webb, B.W., 1994. "k-distributions and weighted-sum-of-gray-gases—a hybrid model". *Heat Transfer*, Vol. 2, pp. 19–24.

Dorigon, L.J., Duciak, G., Brittes, R., Cassol, F., Galarça, M. and França, F.H.R., 2013. "WSGG correlations based on HITEMP2010 for computation of thermal radiation in non-isothermal, non-homogeneous H_2O/CO_2 mixtures". *International Journal of Heat and Mass Transfer*, Vol. 64, pp. 863–873.

Edwards, D.K., Glassen, L.K., Hauser, W.C. and Tuchscher, J.S., 1967. "Radiation heat transfer in nonisothermal nongray gases". *Journal of Heat Transfer*, Vol. 89, No. 3, pp. 219–228.

Fonseca, R.J.C., Fraga, G.C., Coelho, F.R. and França, F.H.R., 2023a. "A wide-band based weighted-sum-of-gray-gases model for participating media: application to H_2O-CO_2 mixtures with or without soot". *International Journal of Heat and Mass Transfer*, Vol. 204, p. 123839.

Fonseca, R.J.C., Fraga, G.C., Coelho, F.R. and França, F.H.R., 2021. "A wide-band formulation for the weighted-sum-of-gray-gases model applied to non-isothermal participating media". In *Proceedings of the 26th International Congress of Mechanical Engineering*. ABCM.

Fonseca, R.J.C., Fraga, G.C. and França, F.H.R., 2023b. "An extension of the wide-band based weighted-sum-of-gray-gases model to high pressure conditions". In *Proceedings of the 10th International Symposium on Radiative Transfer, RAD-23*. Begellhouse.

Fonseca, R.J.C., Fraga, G.C., Silva, R.B. and França, F.H.R., 2018. "Application of the WSGG model to solve the radiative transfer in gaseous systems with nongray boundaries". *Journal of Heat Transfer*, Vol. 140, No. 5, p. 052701.

Fonseca, R.J.C., França, F.H.R. and Fraga, G.C., 2022. "Development and application of a wide-band approach based on the weighted-sum-of-gray-gases model for problems with non-gray walls". In *Proceedings of the 19th Brazilian Congress of Thermal Sciences and Engineering*. ABCM.

Hottel, H.C. and Sarofim, A.F., 1967. *Radiative Transfer*. McGraw-Hill.

Howell, J.R., Mengüç, M.P. and Siegel, R., 2016. *Thermal Radiation Heat Transfer*. CRC press, 6th edition.

Kaminski, D., Fu, X. and Jensen, M., 1995. "Numerical and experimental analysis of combined convective and radiative heat transfer in laminar flow over a circular cylinder". *International Journal of Heat and Mass Transfer*, Vol. 38, No. 17, pp. 3161–3169.

Kez, V., Liu, F., Consalvi, J., Ströhle, J. and Epple, B., 2016. "A comprehensive evaluation of different radiation models in a gas turbine combustor under conditions of oxy-fuel combustion with dry recycle". *Journal of Quantitative Spectroscopy and Radiative Transfer*, Vol. 172, pp. 121–133.

Lathrop, K.D. and Carlson, B.G., 1964. "Discrete ordinates angular quadrature of the neutron transport equation".

Liu, Y., Liu, G., Hu, H. and Kong, B., 2019. "A wavenumber subinterval grouping strategy compatible with non-gray metal wall boundaries used in multi-scale multi-group full spectrum k-distribution gas radiation model". *Applied Thermal Engineering*, Vol. 162, p. 114216.

Mazumder, S. and Modest, M.F., 1999. "A probability density function approach to modeling turbulence–radiation interactions in nonluminous flames". *International Journal of Heat and Mass Transfer*, Vol. 42, No. 6, pp. 971–991.

Modest, M.F., 2013. *Radiative Heat Transfer*. Academic Press.

Modest, M.F. and Haworth, D.C., 2016. *Radiative Heat Transfer in Turbulent Combustion Systems: Theory and Applications*. Springer.

Modest, M.F. and Sikka, K.K., 1992. "The stepwise gray P-1 approximation for multi-dimensional radiative transfer in

molecular-gas—particulate mixtures". *Journal of Quantitative Spectroscopy and Radiative Transfer*, Vol. 48, No. 2, pp. 159–168.

Rothman, L.S., Gordon, I.E., Barber, R.J., Dothe, H., Gamache, R.R., Goldman, A., Perevalov, V.I., Tashkun, S.A. and Tennyson, J., 2010. "HITEMP, the high-temperature molecular spectroscopic database". *Journal of Quantitative Spectroscopy and Radiative Transfer*, Vol. 111, No. 15, pp. 2139–2150.

Selhorst, A.H.B., Fraga, G.C., Coelho, F.R., Bordbar, H. and França, F.H.R., 2022. "A compact WSGG formulation to account for inhomogeneity of H_2O-CO_2 mixtures in combustion systems". *Journal of Heat Transfer*, Vol. 144, No. 7.

Solovjov, V.P., Lemonnier, D. and Webb, B.W., 2013. "Efficient cumulative wavenumber model of radiative transfer in gaseous media bounded by non-gray walls". *Journal of Quantitative Spectroscopy and Radiative Transfer*, Vol. 128, pp. 2–9.

Taine, J., 1983. "A line-by-line calculation of low-resolution radiative properties of CO_2-CO-transparent nonisothermal gases mixtures up to 3000 K". *Journal of Quantitative Spectroscopy and Radiative Transfer*, Vol. 30, No. 4, pp. 371–379.

Wall, T., Stanger, R. and Santos, S., 2011. "Demonstrations of coal-fired oxy-fuel technology for carbon capture and storage and issues with commercial deployment". *International Journal of Greenhouse Gas Control*, Vol. 5, pp. 5–15.

8. RESPONSIBILITY NOTICE

The authors are solely responsible for the printed material included in this paper.